A&A manuscript no.
(will be inserted by hand later)

Your thesaurus codes are:
06 (06.09.1; 06.05.1; 02.05.2)

ASTRONOMY
AND
ASTROPHYSICS
1.2.2008

Solar Models: Influence of Equation of State and Opacity

M. Yıldız[1], **N. Kızıloğlu**[2]

[1] Ege University, Department of Astronomy and Space Sciences, İzmir 35100 , Turkey
[2] Middle East Technical University, Physics Department, Ankara 06531, Turkey

Received September, 1996; accepted January 22, 1997

Abstract. Solar models through evolutionary phases of gravitational contraction, pre-main sequence and MS phases, up to current age 4.5×10^9 *yr.* and 4.57×10^9 *yr.*, were studied adopting different prescriptions for the equation of state (EOS) and different opacity tables.

Old EOS in Ezer's evolutionary code that we adopted in previous studies includes pressure ionization, and degeneracy of electrons. In the present study the EOS is obtained by minimization of the free energy (Mihalas et al. 1990, MHD), and the radiative opacity is derived from recent OPAL tables, implemented by the low temperature tables of Alexander & Ferguson. The results are compared with solar models we computed with different radiative opacities (Cox & Stewart 1970) and different EOS, as with models computed by other authors.

Finally we provide the internal run of the thermodynamic quantities of our preferred solar model which possesses the following characteristics: age 4.50×10^9 *yr.*, initial He abundance by mass 0.285, parameter of the mixing length $\alpha = 1.82$, radius and temperature at the bottom of the convective envelope are $R_b = 0.724\, R_\odot$ and $T_b = 2.14 \times 10^6\, K$, respectively.

Key words: The Sun: interior–solar evolution– equation of state

1. Introduction

Recent improvements concerning radiative opacities and equation of state removed significant discrepancies between observations and theory of stellar evolution. Updated solar models (Turck-Chièze et al. 1993; Charbonnel & Lebreton 1993; Gabriel 1994a; Basu & Thompson 1996) are in good agreement with the solar helioseismic data.

Send offprint requests to: M. Yıldız

In this work models are constructed for the Sun starting when model becomes stable against gravitational contraction, with different EOS and opacities, by using Ezer's stellar evolutionary code (EC) (Ezer & Cameron 1967; Yıldız & Kızıloğlu 1995). EOS of MHD (Mihalas et al. 1990; and references therein) which uses an approach known as chemical picture is based on minimization of the free energy and is applicable for stellar modeling. We have chosen opacity tables of OPAL (Iglesias et al. 1992). Since those tables do not extend to low temperatures, Alexander & Ferguson opacity (1994) is used for outer layers of the stars. The models computed for comparison are obtained using Cox & Stewart (1970) (CS) opacity and EC EOS which takes into account degenerate electrons and pressure ionization in an artificial way. Since OPAL opacity, near the bottom of the convective zone, is larger than the CS opacity by a factor of about two, it strongly affects the structure of the convective zone. In performing the solar calibration, the lower luminosity due to enhancement of the opacity also in radiative regions is balanced by decreasing H (or increasing He) abundance. Thus, the abundance of H by mass may also be significantly altered.

It was shown that the MHD EOS removes significantly the discrepancies between the observational and the theoretical frequencies of the solar oscillations (Christensen-Dalsgaard et al. 1988). However we do not mention about the solar oscillations. The incorporation of the Coulomb interaction in EOS reduces both of the pressure and the energy. To compensate this reduction in pressure, the mean molecular weight per free particle, that is He abundance, becomes smaller, in contrast to the effect of OPAL opacity. The application of MHD EOS requires the calculation of ionization and internal energy of each chemical species. Avoiding the time consuming calculation of the Saha equation for the heavy elements, we use two different methods, namely, Henyey (Gabriel 1994b) method and Gabriel & Yıldız method (1995).

In Sect. 2 we present the basic features of the code. The EOS with its computational method and opacity used in the construction of the solar models are given in Sect 3. Sect. 4 is devoted to the influence of MHD EOS includ-

ing the results of the two methods for the ionization and internal energy of heavy elements. In Sect. 5 we give the results of the solar models with different EOS and opacity.

2. Basics of the Modeling

We solve the four non−linear differential equations of the stellar structure by the method of Newton-Raphson, from center all the way to the surface, with the surface boundary conditions given as

$$L = 4\pi\sigma\, R^2\, T_{eff}^4, \qquad \frac{P_{ph}}{\tau} = \frac{GM}{R^2\kappa} + \frac{1}{2} a\, T_{eff}^4 \tag{1}$$

where P_{ph} is photospheric pressure, τ is the optical depth taken to be 2/3, and the remaining symbols have the usual meaning.

Mass fraction of heavy elements is taken to be 0.019. Chemical abundances of the solar surface found by Anders & Grevesse (1989) are chosen. Nuclear reactions are from Caughlan & Fowler (1988). For convection, classical mixing length theory of Böhm-Vitense (1958) and Schwarzschild criteria are used.

Stellar models are employed mostly in comparative works. Therefore the accuracy of the code is very important. For this reason the code is modified to obtain more accurate models. In order to acquire a higher accuracy, two points derivative of thermodynamic quantities are replaced with quadratic ones. The relative changes of the physical variables become smaller than 10^{-4} for each shell boundaries in the solution of the equation of stellar structure by the Henyey method.

3. Input Physics

3.1. Opacity

In order to test the influence of the uncertainities in the radiative opacities we have used different sets of the opacity. The OPAL opacity is available for the temperatures larger than 6000 K, and implemented by the Alexander & Ferguson opacity table at low temperatures (OA). For the Sun, the transition point ($T =$ 8000 K) is chosen such that it always belongs to convective region in all evolutionary phases of the Sun. So, small discrepancies may not cause any problem in the solution of finite-difference equations. We calculate the opacity by quadratic interpolation in chemical composition, T and R ($R = \rho/T_6^3$).

Model 1 and 2 are obtained using the radiative opacity of CS. The opacity tables include three H-He mixtures in which H/He =4; 1; 0. Required opacity for the solar material is found by logarithmic interpolation between the three sets of the opacity tables.

3.2. Equation of State: Minimization of Free Energy

The free energy is minimized in order to obtain the Saha equation which is required to find the number of particles in each degree of ionization. This is the chemical picture in which atoms and molecules are described as separate entities.

Since Fermi and Bose gases obey different statistics, their free energies, F, are different. But, disregarding signs, they have the same form:

$$F = \Omega + \mu N, \tag{2}$$

$$\Omega = -PV = \mp kT \sum_i \ln(1 \pm e^{(\mu-\epsilon_i)/kT}), \tag{3}$$

where summation is over all quantum states i, μ is the chemical potential, ϵ_i is the energy of this state, and k is the Boltzman constant. For Fermi (Bose) gas upper (lower) sign in Eq. (3) applies. Total number of particles, N, is given by the summation of the average occupation number over all quantum states, n_i.

3.2.1. Degeneracy of Electrons

The free energy of a gas of particles with half integral spin is not as simple as that of the photon gas in those regions of the $\rho - T$ plane where the gas is partially degenerate and partially relativistic. In the region of interest, there is no analytic solutions of the EOS except at some points in which both degeneracy parameter λ ($\lambda = \mu/kT$) and relativistic parameter β ($\beta = kT/mc^2$) have extreme values. Therefore numerical methods should be employed for a semi-relativistic and semi-degenerate gas. As Q_n functions introduced by Guess (1966) are better suited for numerical calculations than Fermi-Dirac functions, we express Ω_e as

$$\Omega_e = -\frac{\pi}{3}\frac{m^4c^5}{h^3} V \left(Q_4 - 4Q_2 + 3Q_0\right). \tag{4}$$

Like Ω_e, the number density of electrons n_e is an implicit function of λ and β. In terms of the functions Q_n it is given as

$$n_e = \frac{N_e}{V} = 2\pi \left(\frac{mc}{h}\right)^3 \left(Q_3 - Q_1\right), \tag{5}$$

where N_e is the number of electrons in volume V. If $\lambda >> 0$ then perfect gas relation is recovered and λ for the non-relativistic region can be given in terms of n_e and T:

$$e^{-\lambda} = \frac{h^3}{2(2\pi mk)^{3/2}} \frac{n_e}{T^{3/2}}, \tag{6}$$

which corresponds to slightly degenerate or non-degenerate case.

Then the energy and the pressure are given by the derivatives of the free energy with respect to the temperature and to the volume, respectively:

$$E_e = \pi \frac{m^4c^5\, V}{h^3} \left(Q_4 + Q_0\right), \tag{7}$$

$$P_e = \frac{\pi}{3}\frac{m^4c^5}{h^3} \left(Q_4 - 4Q_2 + 3Q_0\right). \tag{8}$$

3.2.2. Boltzmann Gas and Partition Function

Free energy for the Boltzmann gas can be written as follows

$$F_b = \sum_{i,j} F_{bi}^j = -kT \sum_{i,j} N_i^j \ln \left[\frac{eV}{N_i^j} \left(\frac{2\pi m_i kT}{h^2} \right)^{3/2} B_i^j \right] . \quad (9)$$

where N_i^j and B_i^j are number of i-type j-times ionized ions in volume V and partition function of these ions, respectively.

Now, energy and pressure can be found for a Boltzman gas by differentiating F_b given above. Since partition function is also a function of temperature and density (due to interaction between particles), its derivatives must also be taken into account:

$$E_b = kT \sum_{i,j} N_i^j \left(\frac{3}{2} - \sum_{m=j+1}^{Z} \frac{I_i^m}{kT} + \frac{\partial \ln U_i^j}{\partial \ln T} \right) , \quad (10)$$

and

$$P_b = kT \sum_{i,j} n_i^j \left(1 - \frac{\partial \ln U_i^j}{\partial \ln \rho} \right) \quad (11)$$

where $n_i^j \equiv N_i^j / V$ and $B_i^j = e^{\epsilon_{i,0}^j / kT} U_i^j$. The second quantity in the parenthesis in Eq.(10) is $\epsilon_{i,0}^j / kT$ where I_i^m is the mth ionization potential of i-type ion

Influence of interaction between atoms (ions) may obliterate some outer states of an atom. Electrons occupying these states are not bounded to the atom any more. This is known as pressure ionization. MHD have shown how to include the effect of pressure ionization into the partition function based on Ünsold's theory (Clayton 1968). According to Ünsold's theory partition function can be written as

$$U_i^j = \sum_k g_{i,k}^j w_{i,k}^j e^{-\chi_{i,k}^j / kT} \quad . \quad (12)$$

where $w_{i,k}^j$ is the survival probability of the state k for a j-times ionized i-type atom with j less electron, $g_{i,k}^j$ and $\chi_{i,k}^j$ are the statistical weight and excitation energy of this state, respectively.

If the survival probability for any state is zero, neither this state nor higher states contribute to the partition function. Apart from thermodynamical consistency the survival probability given by MHD has important advantages. The partition function doesn't explode, and transition from bound to free states is continuous since $w_{i,k}^j$ is continuous.

3.2.3. Coulomb Interaction

At relatively high densities atoms are very close to each other. A bound electron may not preserve its original state under the influence of the Coulomb potential due to other charged particles in the plasma. The Coulomb interaction implies that slight changes occur in the energy and the pressure. An approximate expression for the Coulomb energy is given by Landau & Lifshitz (1969) as

$$E_c = -q_e^3 \left(\frac{\pi}{kTV} \right)^{1/2} \left(\sum_{i,j} N_i^j j^2 \right)^{3/2} = -\frac{1}{2} q_e^2 \frac{\sum_{i,j} N_i^j j^2}{R_D} \quad (13)$$

where q_e is proton charge and R_D is Debye radius. Expression for pressure due to interaction is

$$P_c = -\frac{q_e^3}{3V} \left(\frac{\pi}{kTV} \right)^{1/2} \left(\sum_{i,j} N_i^j j^2 \right)^{3/2} . \quad (14)$$

As seen in Eqs. (13) and (14) both E_c and P_c are negative, since the Coulomb interaction causes a decrease in the energy and the pressure.

3.2.4. Saha Equation

To find equilibrium number of particles it is necessary to minimize the free energy using stoichiometric relations describing ionization (or dissociation) processes. Then the Saha equation is obtained with ionization potential I_k^l of l-times ionized k-type atom:

$$\frac{N_k^{l+1}}{N_k^l} = \frac{U_k^{l+1}}{U_k^l} \exp\Big\{ \lambda - \left\{ I_k^l - 2(l+1) c_2 (N \overline{Z_{eff}^2})^{1/2} \right\} / kT + \sum_{i,j} N_i^j \left(\frac{\partial \ln U_i^j}{\partial N_k^{l+1}} - \frac{\partial \ln U_i^j}{\partial N_k^l} \right) \Big\} \quad . \quad (15)$$

where

$$\overline{Z_{eff}^2} = \frac{1}{N} \sum_{i,j} N_i^j j^2 \quad (16)$$

with N being the total number of particles in the system including electrons.

Two remarks are called for Eq. (15) which includes degeneracy of electrons and the Coulomb interaction. First, any additional term to the free energy appears with its partial derivative with respect to the number density of particles and as an argument of the exponential in the Saha equation. Second, both of the terms coming from the free energies of the degenerate electrons and the Coulomb interaction behave like processes lowering ionization potential. Therefore, some of the early works on EOS (Harris 1964; Graboske et al. 1969) treated ionization potential somehow as a function of the thermodynamical variables.

3.3. Computational Method of EOS

The total energy and pressure of the plasma are the summation of the partial contributions of the effects discussed

in the previous sections and the radiation term. Most of the physical quantities appearing in the equations for energy and pressure of different kinds of gases can be identified, explicitly or implicitly, in terms of number density of electrons. Therefore the EOS is calculated by iterating over the number of moles of electrons per unit mass, N_e (Gabriel 1994b). Then the problem reduces to solve the Saha equation for any given value of N_e.

We implemented the whole procedure in our stellar evolution code in the following way. Starting from the center, an initial guess of N_e is obtained by assuming the complete ionization, that is each species has charge $Z_i q_e$, which is sufficiently accurate for the center of a star. And then, in outer shells, the first guess of N_e is taken as its last computed value in the previous shell, until the surface is reached.

From the value of N_e, the degeneracy parameter $\Lambda = e^{-\lambda}$ is found from Eq. (6). In the transition region $0.0005 < \Lambda < 600.0$, gas is partially degenerate and Λ can be recalculated from the fitting formula of Henyey (Gabriel 1994b; Yıldız 1996).

Because of the low abundance of heavy elements in the solar mixture, probably it is unnecessary for those elements, to calculate the quantities such as partition functions and the number of elements at any degree of ionization, with high accuracy. Only for H and He very precise calculations need to be done.

In order to save computer time, all that is needed is to calculate the effective degree of ionization (i.e., effective charge of each element)

$$Z_{eff,i} = \frac{\sum_j N_i^j j}{N_i} \quad . \tag{17}$$

Then, there is no need to solve the Saha equation. Two methods are used to compute the effective charges of ^{12}C, ^{14}N, ^{16}O, ^{20}Ne and the binding energies of these atoms (ions). The first one is Henyey's fitting method (Gabriel 1994b; Yıldız 1996) which uses $N_e kT$ and the chemical potential of electron μ_e as input parameters. The second method is due to Gabriel & Yıldız (1995), which is similar to Henyey's method but more precise. It takes into account Debye radius as an additional parameter.

Since heavy elements are rare in the atmospheres of the stars only the molecules of hydrogen, H_2, H_2^+, and H^- are considered. The abundance and the energies of these molecules are solved by the method of Vardya (1961).

4. Influence of MHD EOS

In order to compare the results and the influence of MHD EOS, the required density, temperature and chemical composition are taken from a model of the present Sun (Model A, see Table 1). Henyey method is used for ionization of heavy elements, unless stated otherwise.

Contribution of the Coulomb interaction, the degeneracy of the electrons and derivative of the partition function to the total pressure can be seen in Fig.1. For the Model A $P/(P-P')$ is plotted with respect to $\log(T)$ of temperature from surface to the center throughout the solar model, where P is the total pressure, and P' is any of fractional contribution to the pressure. Thin solid line is for the Coulomb pressure. The ratio is less than or equal to one, since the Coulomb term causes a decrease in pressure. At the surface the Coulomb pressure is zero. As the temperature and the density, and therefore the degree of ionization increase, fractional change becomes a few percent. Contribution of the Coulomb potential to the total pressure is maximum (6%) between $\log(T) = 4.6$ and 4.7, at which point the most abundant species (hydrogen and helium) are completely and singly ionized, respectively. This means that the Debye radius is sufficiently small. As the temperature and the density increase the contribution becomes smaller, until partial degeneracy of the electrons sets in near the center of the Sun.

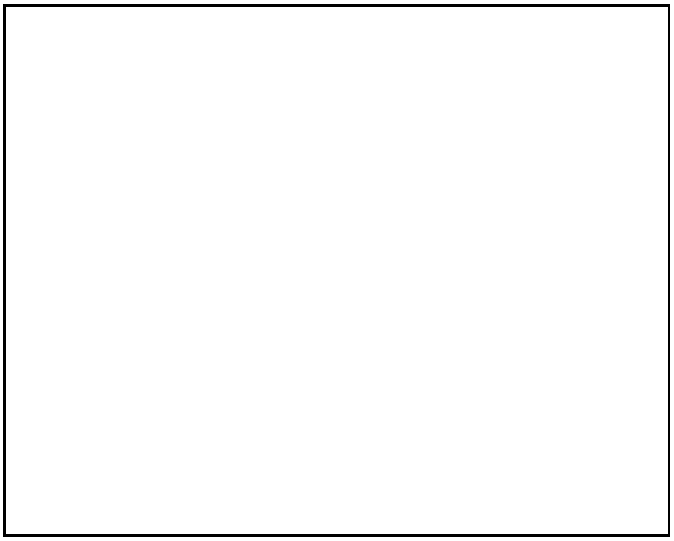

Fig. 1. The fractional contribution to the pressure due to Coulomb interaction, degeneracy of electrons and derivative of the partition functions of H, He, and He^+ with respect to density, is plotted as a function of the logarithm of the temperature for a selected solar model (case A below).

The pressure of the degenerate-electrons calculated by Henyey fitting formula (also calculated by method of Yıldız & Eryurt-Ezer (1992) using Guess functions, the difference is less than 0.01%), represented by dots, deviates from one at the central part. Here $N_e kT$ is subtracted from the total electron pressure. At the center of the Sun degeneracy parameter (λ) is equal to -1.559 which implies a slight degeneracy, and the contribution of degenerate-electrons is about 2%.

Thick solid line in Fig.1. is a superposition of three Gaussian curves. From left to right, the first one is dominantly the density derivative of hydrogen partition function which is maximum ($\approx$ 0.5%) at $\log(T) \approx 4.5$. Sec-

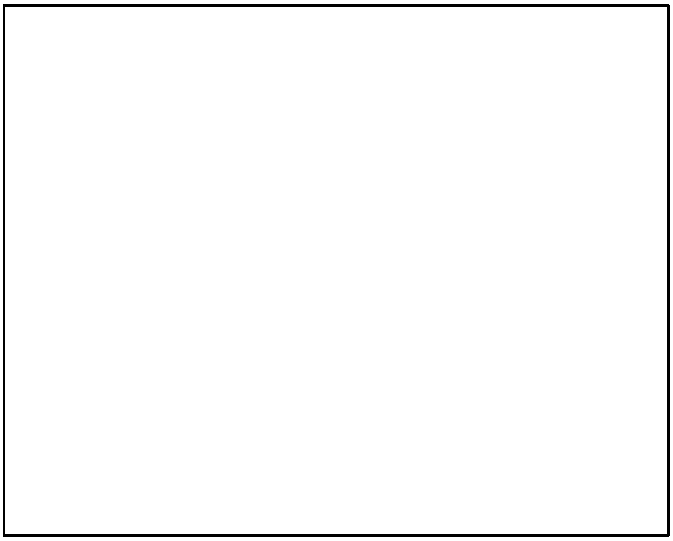

Fig. 2. The run of the effective charge of several elements as a function of the logarithm of the temperature in the model of Fig. 1. The Saha equation is solved for H and He, and Henyey's method is used for heavy elements.

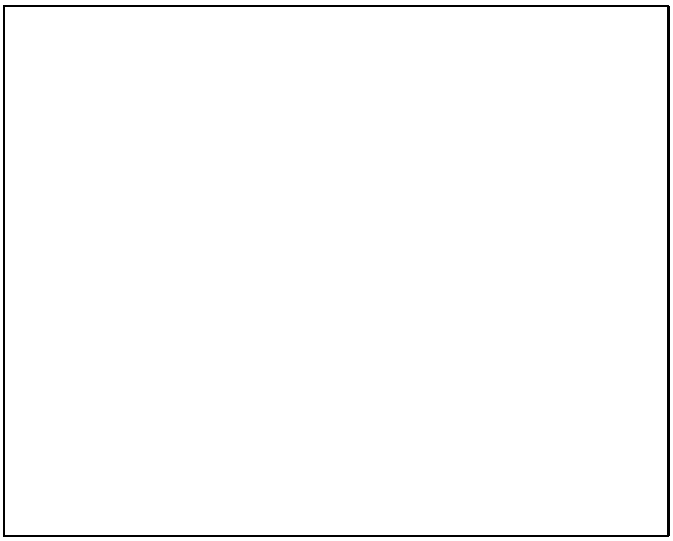

Fig. 3. The run of the effective charge of several elements as a function of the logarithm of the temperature in the model of Fig. 1. The Saha equation is solved for H and He, and the method of Gabriel & Yıldız (1995) is used for heavy elements.

ond one is due to the density derivative of He partition function, which is maximum at about $\log(T) \approx 4.75$ and its contribution to the total pressure is less than 1%. Last one is due to the density derivative of He^+ partition function, which is non-zero in an important part of the solar interior but with a lower contribution to the total pressure than the others. The base temperature of the convective zone in the Model A is about $2.14 \times 10^6\ K$. This corresponds to a point ($\log(T) = 6.3$) at which He^+ starts to appear.

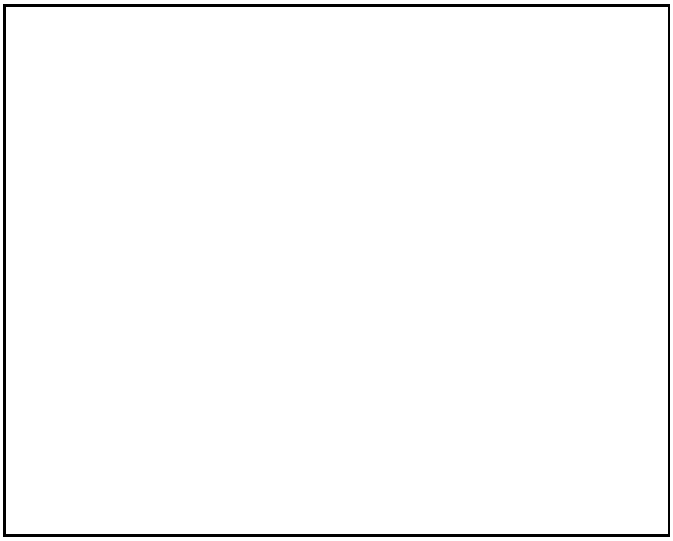

Fig. 4. The ratio of adiabatic gradients resulting from MHD EOS with Gabriel & Yıldız (1995) (solid line) and with Henyey (dots) methods for ionization of heavier elements, to that obtained adopting the EOS of old routine in Ezer's code (EC) for the selected model of Fig. 1.

The Saha equation, Eq (15), is solved exactly for H and He. Results obtained from Henyey method, the effective charges divided by the atomic numbers of each element, throughout the Model A, are given in Fig.2. Due to its low ionization potential hydrogen (solid line with asterisks) is rapidly completely ionized (at $\log(T) \approx 5.2$). For the effective charge of He (solid line with circle) two phases are seen. Even at the center, none of the heavier elements, C (solid line), N (dashed line), O (solid line with triangle), Ne (dashed line with asterisks) are completely ionized. Owing to rough calculation, each line of the heavy elements cross each other near the center. On the other hand, at the center the radiation and the gas pressure (and energy) are sufficiently large, therefore the computed values are within an acceptable range. This is not the case at the surface where binding energy has an important role in the total energy. While H and He are neutral, each of the heavier elements is in the state of first ionization.

A physically more reliable method is that of Gabriel & Yıldız (1995). As seen in Fig.3, at the middle of the Sun, ionization degrees of the heavier elements are a little bit smaller than, but comparable to those given in Fig.2. At the center and at the surface, the values of ionization degree are not in contradiction with the basic truths of atomic physics. All atoms are neutral at the surface. Ionization of C starts before H, and ionization of N, O,and Ne starts after H but before He, as expected from the atomic physics.

The effect of the MHD EOS on the adiabatic gradient is shown in Fig.4. There we plot the ratio of the adiabatic

Table 1. Comparison of the present solar models with different EOS, opacities and data of the Sun.

Models	Y	α	$R_c/R_\odot$	$T_b/10^6$	T_{eff}	$T_c/10^6$	ρ_c	X_c	$P_c/10^{17}$
1 (CS EC D1)	0.224	1.32	0.19	1.24	5804	15.00	136.4	0.438	2.244
2 (CS MHD+H D1)	0.205	1.46	0.20	1.31	5794	14.91	132.0	0.478	2.147
3 (OA EC D1)	0.302	1.57	0.27	2.07	5799	15.80	151.9	0.324	2.342
4 (OA MHD+H D1)	0.284	1.76	0.27	2.11	5797	15.70	149.3	0.338	2.271
A (OA MHD+GY D1)	0.285	1.82	0.276	2.14	5799	15.70	147.1	0.345	2.269
B (OA MHD+H D1)	0.285	1.78	0.277	2.15	5799	15.69	147.5	0.343	2.267
C (OA MHD+GY D2)	0.283	1.82	0.276	2.16	5792	15.67	148.6	0.339	2.270
CL (1993)	0.278	1.66	0.281	2.13		15.56	150.7		
BU (1988)	0.271		0.277	2.11		15.62	148	0.341	2.290
TCCD (1988)	0.275	2.11	0.270	2.04		15.52	147.2		
CGK (1989)	0.291	1.89	0.286	2.29	5770	15.68	162.4	0.352	2.2 78
SBF (1990)	0.278	2.07	0.260	1.96		15.42	146.6		
LD (1988)	0.278	2.16	0.265	2.02	5781	15.54	148.0	0.352	2.278
CDR (1996)	0.265	1.77	0.274	2.10		15.45	147.2	0.372	

gradient resulting from the Gabriel & Yıldız (solid line) and from the Henyey method (dotted line) to the value obtained with EC EOS are given. Both are larger than the old gradient, and three peaks correspond ionization zones of H, He and He^+.

5. Results and Discussion

Recently we have gathered very important information about the internal structure of the Sun by helioseismological investigations. Distance of the convective zone from the center of the Sun is determined from p-mode oscillations as $0.713 \pm 0.003\ R_\odot$ by Christensen-Dalsgaard et al. (1991). Photospheric abundance of He by mass is found as 0.242 ± 0.003 (Hernandez & Christensen-Dalsgaard 1994). There are several attempts to determine the central density of the Sun from helioseismological data. Results obtained by Dziembowski et al. (1994) are in between $130-150\ g\ cm^{-3}$, while Gough & Kosovichev (1988) quote $\approx 160\ g\ cm^{-3}$ and Vorontsov & Shibahashi (1991) quote a range of $110 - 115\ g\ cm^{-3}$.

Two sets of the solar data are used in the calculations. In one set (D1), the age of the Sun is taken as $4.5\times10^9\ yr.$, and its luminosity and radius are $3.90 \times 10^{33}\ erg\ s^{-1}$ and $6.951 \times 10^{10}\ cm$, respectively. In the other set (D2) (case C below), the luminosity and the age of the Sun are taken from Bahcall et al. (1995), namely $L_\odot = 3.8440 \times 10^{33}\ erg\ s^{-1}$ and $t_\odot = 4.57\times10^9\ yr$. The radius of the Sun is $R_\odot = 6.9598 \times 10^{10}\ cm$ (Sackmann et al. 1993). In both of the sets the solar mass is $1.985 \times 10^{33}\ g$.

For different combinations of EOS's and opacities and for different solar data, starting from threshold of stability point at which gravitational and internal energies are nearly the same, we constructed a series of evolutionary models for the Sun. Each model given in Table 1 is obtained by changing initial mass fraction of hydrogen, helium and convective parameter α, in order to fit the Sun's luminosity and radius to the present data, with different accuracies. The first column in Table 1 represents the initial abundance of He by mass, and α is given in the second column. The depth of the convective zone in terms of solar radius, $R_c/R_\odot$, is shown in the third column, and base temperature of the convective zone, T_b, is in the fourth column. Last five columns are the effective temperature (T_{eff}), the central temperature (T_c), density(ρ_c), abundance of hydrogen by mass at the center (X_c), and the central pressure (P_c), respectively (in cgs). All the models, except Model C, is with D1. The first three models are constructed with an accuracy of a few percent, and the fourth model with an accuracy of 0.5%. Models A, B and C are more precise models (accuracy is 10^{-4}). The difference between the Model A and the Model B is the method of heavy element ionization. The latter (also Model 4) uses Henyey's method (MHD+H), the former is obtained by the method of Gabriel & Yıldız (MHD+GY) as the Model C.

When we compare each of the first four models with the model of the same EOS but different opacity (Model 1 with 3, and Model 2 with 4), it is seen that OA opacities strongly influence the structure of the Sun. The enhancement of the opacity (OPAL) below the convective zone enlarges the zone's size toward the center of the Sun. When MHD is used, OA opacities enlarge the convective zone by about 40%, and by 35% if EC EOS is used. Increase in base temperature of convective zone is about 61% with MHD EOS and 67% with EC EOS whenever OA opacities are employed in place of CS opacity. While He abundance by mass is exceeding the helioseismological result, the central density is about $150\ g\ cm^{-3}$, and the base temperature of the convective zone is larger than $2 \times 10^6\ K$ in the models with OA. Because of increase in opacity, less energy reaches the surface. This is compensated by an increase in

Table 2. The present Sun model (Model A) with OPAL opacity and MHD EOS by using method of Gabriel and Yıldız for ionization of heavy elements

Sh.n	$M/M_\odot$	$R/R_\odot$	ρ	T	P	E	$L/L_\odot$	H
1	0.0000	0.000	.1471E+3	.1570E+8	.2269E+18	.2289E+16	0.000	.3455
7	0.0004	0.016	.1446E+3	.1560E+8	.2232E+18	.2290E+16	0.004	.3518
17	0.0017	0.019	.1436E+3	.1557E+8	.2217E+18	.2291E+16	0.007	.3543
41	0.0022	0.028	.1397E+3	.1542E+8	.2158E+18	.2292E+16	0.021	.3640
66	0.0074	0.042	.1309E+3	.1510E+8	.2028E+18	.2301E+16	0.066	.3889
106	0.0550	0.089	.9411E+2	.1355E+8	.1470E+18	.2321E+16	0.368	.5126
126	0.2019	0.155	.5372E+2	.1100E+8	.7553E+17	.2089E+16	0.804	.6373
133	0.2807	0.182	.4166E+2	.1002E+8	.5442E+17	.1941E+16	0.901	.6636
155	0.5582	0.279	.1539E+2	.7289E+7	.1490E+17	.1438E+16	0.996	.6921
179	0.7825	0.393	.4271E+1	.5241E+7	.2972E+16	.1036E+16	1.000	.6959
219	0.9424	0.593	.5375E+0	.3195E+7	.2281E+15	.6330E+15	1.000	.6962
236	0.9701	0.683	.2346E+0	.2511E+7	.7823E+14	.4977E+15	1.000	.6962
256	0.9787	0.724	.1659E+0	.2144E+7	.4720E+14	.4245E+15	1.000	.6962
280	0.9912	0.808	.8149E−1	.1340E+7	.1444E+14	.2634E+15	1.000	.6962
298	0.9958	0.857	.4752E−1	.9381E+6	.5878E+13	.1831E+15	1.000	.6962
356	0.9994	0.933	.1265E−1	.3927E+6	.6457E+12	.7441E+14	1.000	.6962
369	0.9996	0.945	.9133E−2	.3174E+6	.3747E+12	.5947E+14	1.000	.6962
389	0.9998	0.961	.5046E−2	.2167E+6	.1394E+12	.3937E+14	1.000	.6962
409	0.9999	0.970	.3053E−2	.1589E+6	.6090E+11	.2753E+14	1.000	.6962
425	0.9999	0.976	.1993E−2	.1246E+6	.3067E+11	.2005E+14	1.000	.6962
442	1.0000	0.981	.1345E−2	.1012E+6	.1656E+11	.1463E+14	1.000	.6962
458	1.0000	0.985	.8592E−3	.8004E+5	.8222E+10	.9747E+13	1.000	.6962
475	1.0000	0.987	.5616E−3	.6345E+5	.4179E+10	.6144E+13	1.000	.6962
493	1.0000	0.990	.3518E−3	.4986E+5	.2000E+10	.3096E+13	1.000	.6962
512	1.0000	0.992	.2014E−3	.3948E+5	.8721E+09	.3266E+12	1.000	.6962
522	1.0000	0.993	.1454E−3	.3527E+5	.5502E+09	−.9956E+12	1.000	.6962
533	1.0000	0.994	.1043E−3	.3179E+5	.3475E+09	−.2183E+13	1.000	.6962
543	1.0000	0.995	.7647E−4	.2910E+5	.2282E+09	−.3169E+13	1.000	.6962
563	1.0000	0.996	.3947E−4	.2464E+5	.9505E+08	−.4962E+13	1.000	.6962
583	1.0000	0.997	.2024E−4	.2139E+5	.4031E+08	−.6460E+13	1.000	.6962
594	1.0000	0.997	.1433E−4	.2002E+5	.2607E+08	−.7143E+13	1.000	.6962
603	1.0000	0.998	.1045E−4	.1892E+5	.1756E+08	−.7723E+13	1.000	.6962
613	1.0000	0.998	.7633E−5	.1792E+5	.1188E+08	−.8267E+13	1.000	.6962
623	1.0000	0.998	.5036E−5	.1674E+5	.7103E+07	−.8944E+13	1.000	.6962
643	1.0000	0.999	.2610E−5	.1508E+5	.3158E+07	−.9943E+13	1.000	.6962
663	1.0000	0.999	.1296E−5	.1348E+5	.1325E+07	−.1096E+14	1.000	.6962
674	1.0000	1.000	.8965E−6	.1266E+5	.8333E+06	−.1150E+14	1.000	.6962
694	1.0000	1.000	.4730E−6	.1108E+5	.3607E+06	−.1250E+14	1.000	.6962
705	1.0000	1.000	.3356E−6	.9903E+4	.2195E+06	−.1311E+14	1.000	.6962
715	1.0000	1.000	.2679E−6	.8210E+4	.1407E+06	−.1363E+14	1.000	.6962
716	1.0000	1.000	.2658E−6	.8030E+4	.1363E+06	−.1366E+14	1.000	.6962
717	1.0000	1.000	.2642E−6	.7829E+4	.1320E+06	−.1370E+14	1.000	.6962
727	1.0000	1.000	.2421E−6	.6432E+4	.9894E+05	−.1387E+14	1.000	.6962
739	1.0000	1.000	.1682E−6	.5799E+4	.6197E+05	−.1393E+14	1.000	.6962

He abundance. The convective parameter alpha increases by about 30%, when OA is employed in place of CS.

If we compare Model 1 with 2, and Model 3 with 4, it becomes obvious that the depth and the base temperature of the convective zone is not very sensitive to the EOS. The values of He abundance and α are changed by EOS. Incorporation of the Coulomb interaction reduces the energy and pressure by some fraction. In order to compensate this reduction in pressure, mass fraction of He (or molecular weight per free particle) decreases by about 6% in case of CS, and 10% in case of OA opacities. The only difference between the ways that Model A (Gabriel & Yıldız) and B (Henyey) are obtained, is the calculation method of the ionization of heavy elements and their internal energies. There are small differences between these models. The convective parameter α of Model A is a little bit larger

than that of Model B, since the pressure scale height (the number density of electrons) of Model A in outer layers is less than that of Model B.

The small differences between Models B and 4 are due to low accuracy of Model 4. The Models A (D1) and C (D2) have different solar data. The Model C has lower luminosity and higher age than the Model A.

In Table 1, we also give models constructed by Charbonel & Lebreton (CL) (1993), Bahcall & Ulrich (BU) (1988), Turck-Chieze et al. (TCCD) (1988), Cox et al. (CGK) (1989) , Sackmann et al. (SBF) (1990), Lebreton & Däppen (LD) (1988), and Ciacio et al. (CDR)(1996). Similar to our models, all the models obtained by different authors are standard models, that is there is no rotation, no diffusion process and magnetic field is negligible. Except model of CGK, the initial mass fraction of He in Models A, B and C is a little bit larger than those found by other researchers. The extreme model of CGK, which has the largest value of He mass fraction, base temperature of the convective zone, and the central temperature, has an age of $4.66 \times 10^9\ yr$. The EOS of CGK is very similar to EC EOS, and Iben's fitting formula (1975) is used for opacity. The model of CDR which has the same solar data as Model C except the solar mass and heavy element abundance, is obtained by using both the EOS and the opacity of OPAL. The significant difference between these two models is in He abundance due to their data of high solar mass and low metallicity. The other models take the age of the Sun as $4.6 \times 10^9\ yr$. Therefore, their He mass fractions are closer to, but less than, that of our models with OA and MHD EOS. Almost all the models use the same nuclear reaction rates of Caughlan & Fowler. Model of CL, which uses OPAL opacity and tables of MHD EOS, is close to our best models. There is a small difference in the value of α (the difference in He mass fraction is due to different age of the Sun). This difference stems possibly from their different heavy element abundance and low opacity table. They use different initial mixture for heavy elements. Model of BU includes the Coulomb interaction in EOS and the Los Alamos Opacity (Cox et al. 1991).

The physical variables which determine the structure of the Sun is summarized in Table 2. These values (in cgs) are from the Model A which has the accuracy of 10^{-4} and is obtained by using MHD+GY and recent opacities. For accuracy of the model, number of shells is increased to 739, during the evolution. The energy that the Sun radiates is produced within the inner 0.25 $M_\odot$ core. Convective zone is between shells 256 and 727, where radiative temperature gradient exceeds adiabatic temperature gradient. Its mass is only 2% of the total mass of the Sun, and its distance to the center is $0.724 R_\odot$. The total internal energy in outer shells is negative, since binding energy of an atom having electronic configuration is considered negative.

Our conclusion is that solar models obtained by MHD EOS and OPAL opacities are in closer agreement with the results the helioseismology. The remaining small differences can be removed by taking into consideration the diffusion process of He and heavy elements. With MHD EOS and OPAL opacity, and with diffusion process, Basu & Thompson (BT) (1996) gives the distance from bottom of the convective zone to the center as 0.714 $R_\odot$. When one incorporates diffusion processes, Bahcall et al. (1995) emphasize that the decrease in mass fraction of He is about 10% which gives better agreement with the observation. From Table 1, one sees that the main effect upon the initial He abundance is provided by the adoption of the recent opacities which tend to increase the abundance, while the MHD EOS has a smaller effect in the opposite direction

Structure of the Sun is not very sensitive to the methods of Henyey (Model B) and Gabriel & Yıldız (Model A) for the ionization of heavy elements. But the method of Gabriel & Yıldız is better than Henyey method for rapid fitting processes, and, near the surface of the Sun, it gives neutral heavy elements as expected.

Acknowledgements. We thank Dilhan Ezer-Eryurt and Maurice Gabriel for their valuable suggestions, comments and discussion.

References

Alexander D.R., Ferguson J.W.,1994, ApJ 437, 879.
Anders E., Grevesse N., 1989, Geoc. Cos. Act. 53, 197.
Bahcall J.N., Ulrich R.K., 1988, Rev. Mod. Phys. 60, 297.
Bahcall J.N., Pinsonneault M.H., Wasserburg G.J., 1995, Rev. Mod. Phys. 67, 781.
Basu S., Thompson M.J., 1996, A&A 305, 631.
Böhm-Vitense E., 1958, Zs. Ap. 46, 108.
Caughlan G.R., Fowler W.A., 1988, Atomic Data and Nuclear Data Tables 40, 283.
Charbonnel C., Lebreton Y., 1993, A&A 280, 666.
Christensen-Dalsgaard J., Gough D.O., Lebreton Y., 1988, Nature, 336, 634.
Christensen-Dalsgaard J., Gough D.O., Thompson M.J., 1991, ApJ 378, 413.
Ciacio F., Degl'Innocenti S., Ricci B., 1996, artro–ph/9605157.
Clayton D.D., 1968, Principles of Stellar Evolution and Nucleosyntesis, McGraw-Hill, Inc..
Cox J.P., Guzik J.A., Kidman R.G., 1989, ApJ 342, 1187
Cox A.N., Livingston W.C., Matthews M.S., 1991, Solar Interior and Atmosphere, The University of Arizona Press, Tucson, and references therein.
Cox A.N., Stewart J.N., 1970, ApJS 19, 243.
Dziembowski W.A., Goode P.R., Pamyatnykh A.A., Sienkiewicz R., 1994, ApJ 432, 417.
Ezer D., Cameron A.G.W., 1967, Can. J. Phys. 45, 3461.
Gabriel M., 1994a, A&A 292, 281.
Gabriel M., 1994b, private communications.
Gabriel M., Yıldız M., 1995, A&A 299, 475.
Gough D.O., Kosovichev A.G., 1988. In. Rolfe E.J. (ed) Seismology of the Sun and Sun-Like stars, ESA SP-286, p195.
Graboske Jr., H.C., Harwood D.J., Rogers F.J., 1969, Phys. Rev. 186, 210.
Guess A.W., 1966, *The Degenerate Gas*, Advances in Astron. Astrop. 4, 153.
Harris G.M., 1964, Phys. Rev. 133, A427

Hernandez F.P., Christensen-Dalsgaard J., 1994, MNRAS 378, 413.
Iben I.Jr., 1975, ApJ 196, 525.
Iglesias C.A., Rogers F.J., Wilson B.G., 1992, ApJ 397, 717.
Landau L.D., Lifshitz E.M., 1969, Statistical Physics, Addison-Wesley Pub. Comp..
Lebreton Y., Däppen W., 1988. In Rolfe E.J. (ed) Seismology of the Sun and Sun-Like Stars, ESA SP-286, p661.
Mihalas D., Hummer D.G., Mihalas B.W., Däppen W., 1990, ApJ 350, 300.
Sackmann I.J., Boothroyd A.I., Fowler W.A., 1990, ApJ 345, 1022.
Sackmann I.J., Boothroyd A.I., Kraemer K.E., 1993, ApJ 418, 457.
Turck-Chièze S., Cahen S., Caseé M., Doom C., 1988, ApJ 60, 297.
Turck-Chièze S., Däppen W., Fossat E., et al., 1993, Phys. Rep. 230, 57.
Vardya M., 1961, ApJ 133, 107.
Vorontsov S.V., Shibahashi H., 1991, PASJ 43, 739.
Yıldız M., 1996, in *Evolution and Structure of the Sun and Low Mass Stars- Influence of EOS by Minimization of Free Energy Method and of OPAL Opacity*, Ph. D. Thesis, Middle East Technical University.
Yıldız M., Eryurt-Ezer D., 1992, Ap&SS 190, 233.
Yıldız M., Kızıloğlu N., 1995. In Noels A. et al. (eds) Proc. 32nd Liège Int. Astrop. Coll., Stellar Evolution: What Should Be Done, p385.

This article was processed by the author using Springer-Verlag LaTeX A&A style file *L-AA* version 3.

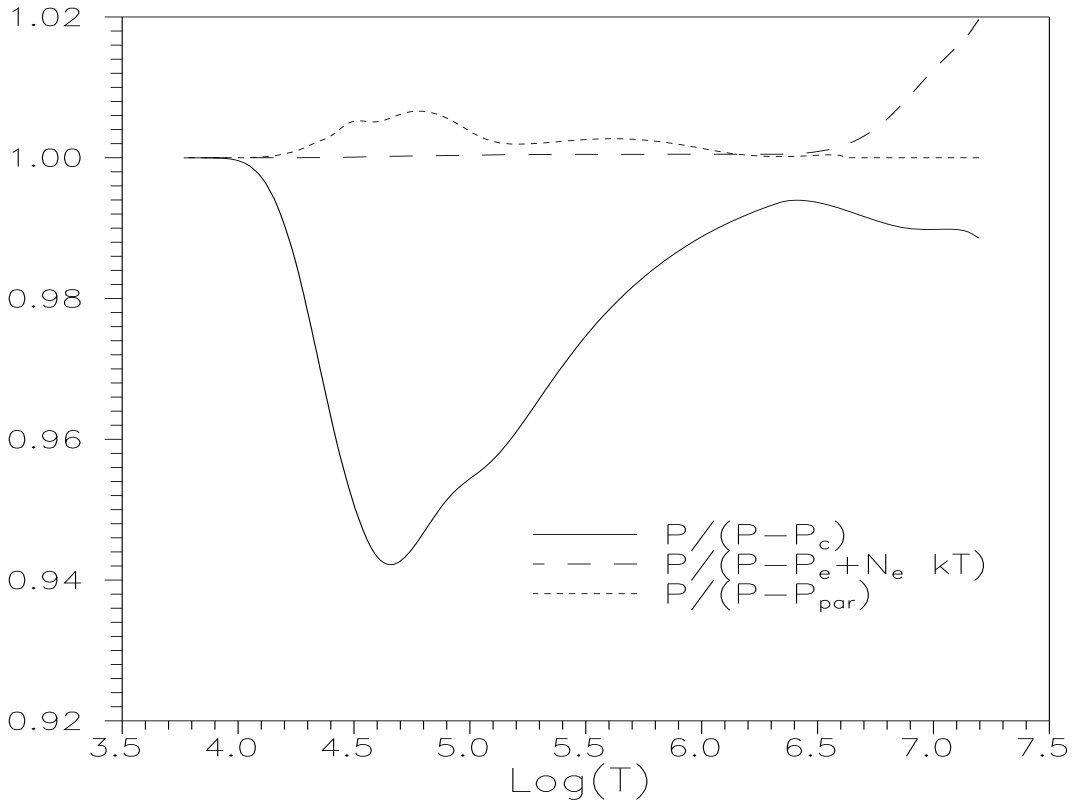
1.02
1.00
0.98
0.96
0.94
0.92
3.5
4.0
4.5
5.0
5.5
6.0
6.5
7.0
7.5
Log(T)
P/(P−P_c)
P/(P−P_e+N_e kT)
P/(P−P_par)

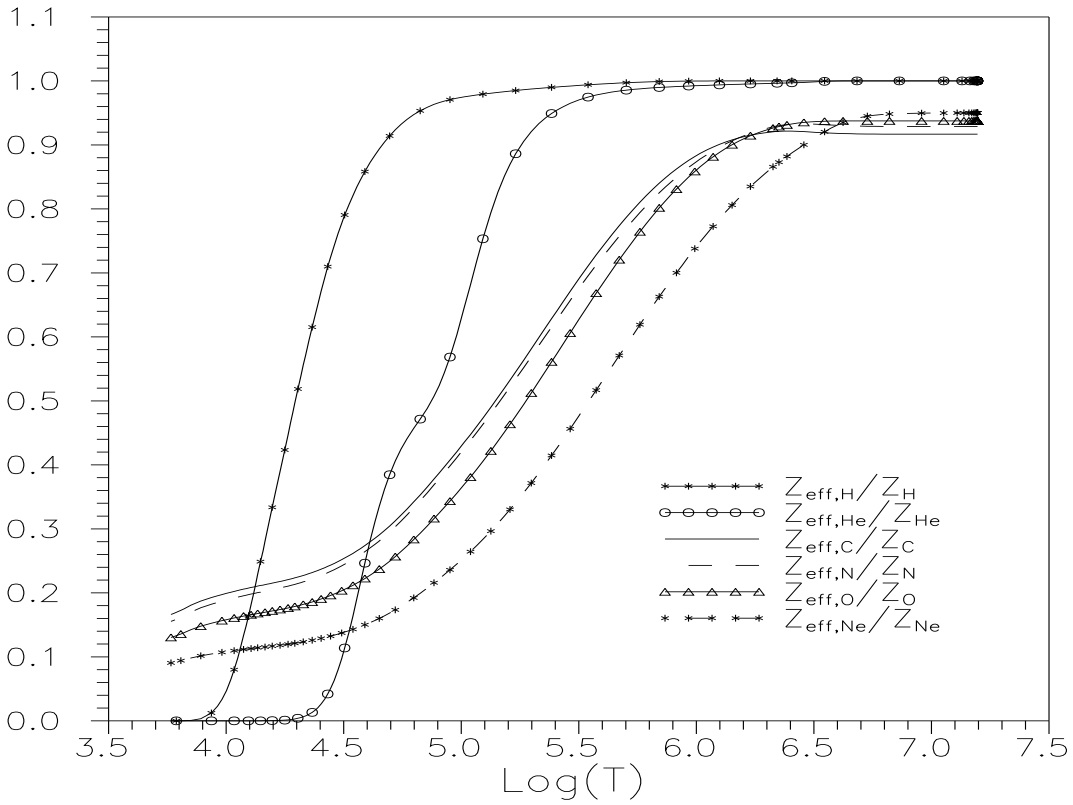
1.1
1.0
0.9
0.8
0.7
0.6
0.5
0.4
0.3
0.2
0.1
0.0
3.5
4.0
4.5
5.0
5.5
6.0
6.5
7.0
7.5
Log(T)
Z eff,H / Z H
Z eff,He / Z He
Z eff,C / Z C
Z eff,N / Z N
Z eff,O / Z O
Z eff,Ne / Z Ne

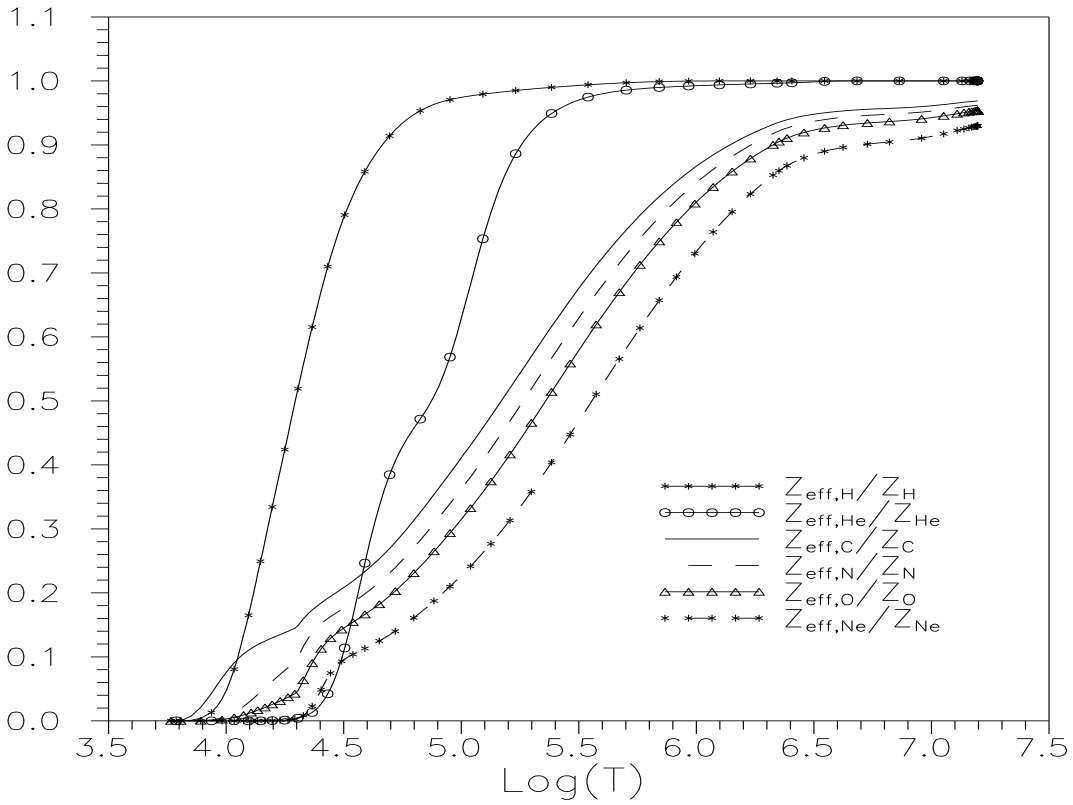
1.1
1.0
0.9
0.8
0.7
0.6
0.5
0.4
0.3
0.2
0.1
0.0
3.5
4.0
4.5
5.0
5.5
6.0
6.5
7.0
7.5
Log(T)
Z eff,H / Z H
Z eff,He / Z He
Z eff,C / Z C
Z eff,N / Z N
Z eff,O / Z O
Z eff,Ne / Z Ne

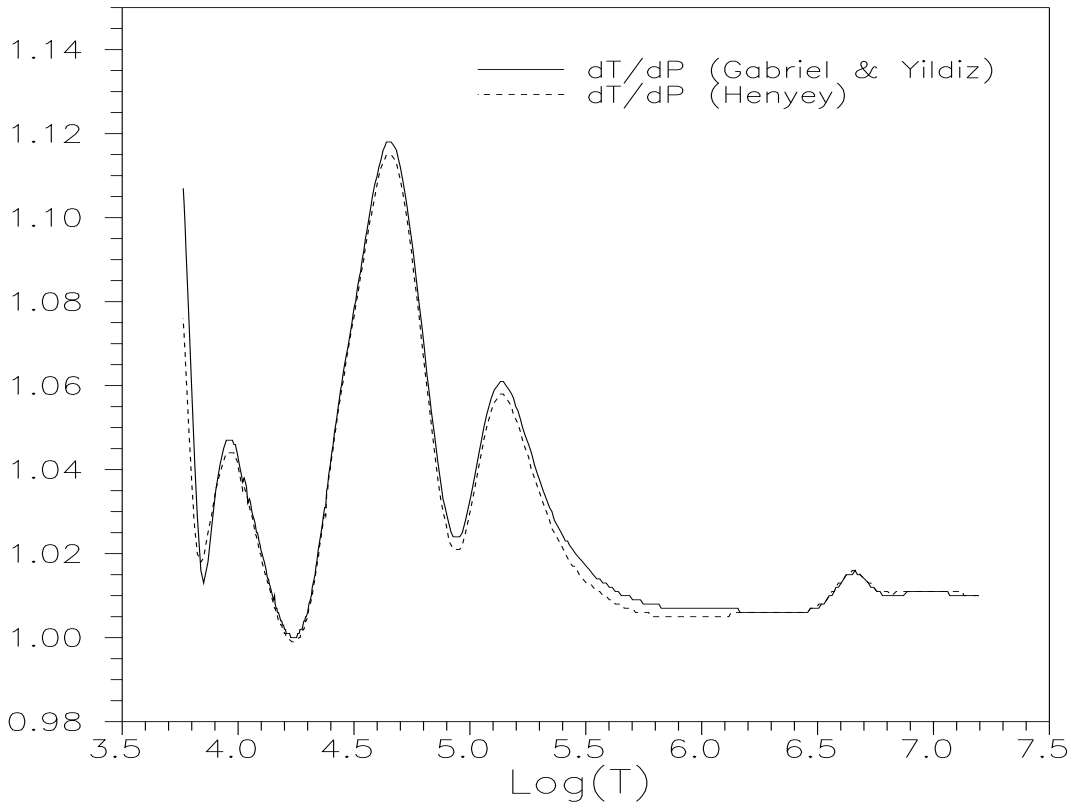
dT/dP (Gabriel & Yildiz)
dT/dP (Henyey)
1.14
1.12
1.10
1.08
1.06
1.04
1.02
1.00
0.98
3.5
4.0
4.5
5.0
5.5
6.0
6.5
7.0
7.5
Log(T)